J Mater Sci (2011) 46:2001–2008
DOI 10.1007/s10853-010-5191-z

Compositional characterization of nickel silicides by HAADF-STEM imaging

E. Verleysen · H. Bender · O. Richard · D. Schryvers · W. Vandervorst

Received: 12 July 2010 / Accepted: 15 December 2010 / Published online: 7 January 2011

Abstract A methodology for the quantitative compositional characterization of nickel silicides by high angle annular dark field scanning transmission electron microscopy (HAADF-STEM) imaging is presented. HAADF-STEM images of a set of nickel silicide reference samples Ni_3Si, $Ni_{31}Si_{12}$, Ni_2Si, NiSi and $NiSi_2$ are taken at identical experimental conditions. The correlation between sample thickness and HAADF-STEM intensity is discussed. In order to quantify the relationship between the experimental *Z*-contrast intensities and the composition of the analysed layers, the ratio of the HAADF-STEM intensity to the sample thickness or to the intensity of the silicon substrate is determined for each nickel silicide reference sample. Diffraction contrast is still detected on the HAADF-STEM images, even though the detector is set at the largest possible detection angle. The influence on the quantification results of intensity fluctuations caused by diffraction contrast and channelling is examined. The methodology is applied to FUSI gate devices and to horizontal TFET devices with different nickel silicides formed on source, gate and drain. It is shown that, if the elements which are present are known, this methodology allows a fast quantitative 2-dimensional compositional analysis.

This paper has been presented as part of the European Materials Research Society E-MRS 2010 Spring Meeting Symposium Q "Quantitative Electron Microscopy for Research and Industry".

E. Verleysen (✉) · H. Bender · O. Richard · W. Vandervorst
Imec, Kapeldreef 75, 3001 Leuven, Belgium
e-mail: eveline.verleysen@imec.be

E. Verleysen · W. Vandervorst
Instituut voor Kern-en Stralingsfysica, K. U. Leuven, Celestijnenlaan 200D, 3001 Leuven, Belgium

D. Schryvers
EMAT, Universiteit Antwerpen, Groenenborgerlaan 171, 2020 Antwerpen, Belgium

Introduction

A wide range of nickel silicide phases with different electrical properties exists [1]. These nickel silicide phases have important applications in the current microelectronics technology. NiSi is used in CMOS devices to lower the interfacial contact resistance between the metal contacts and the source, drain and gate regions [2]. Different nickel silicide phases are explored as potential gate electrodes in fully silicided (FUSI) gate structures [3, 4]. It is generally observed that the nickel silicide phases grow sequentially in thin film reactions [5]. However, for very thin films the diffusivity of nickel can be altered due to the contribution of grain boundary diffusion, or due to the presence of dopants [5]. This can change the reaction kinetics, or even the reaction paths. Furthermore, the formation and dissolution of transient phases in narrow temperature ranges at early stages of the nickel silicidation reaction have been reported [6]. It is clear that control of nickel silicide phases in device structures is critical. Therefore, it is important to be able to perform a fast and accurate quantitative analysis that reveals the 2-dimensional distribution of the different phases present. In this article, we report a methodology for the quantitative compositional 2D characterization of nickel silicides by HAADF-STEM imaging.

In HAADF-STEM, a (sub-)nanometer-sized illuminating electron probe scans over the sample, and the signals produced by the scattering of the electrons can be detected and displayed as a function of the illuminating probe position [7]. A high angle annular detector is used to collect the scattered electrons. Since nickel silicide layers in

scaled CMOS devices are only 10–20 nm thick, high spatial resolution is essential for local phase identification. In HAADF-STEM, the spatial resolution is mainly controlled by the nanosized illuminating probe, down to 0.1 nm in high-resolution STEM mode, allowing the direct visualisation of the atomic column positions if the imaging is performed along a crystal zone axis [8]. As the nickel silicides are generally polycrystalline, such imaging is not possible over the full area of the device structures. In this study, a larger probe is used instead (1–2 nm), which results in an averaged contrast over the atom positions.

It is possible to combine HAADF-STEM imaging with techniques such as electron energy loss spectroscopy (EELS) and energy dispersive X-ray spectroscopy (EDS). EELS and EDS analyses on nickel silicides are reported before [9, 10].

The image intensity in HAADF-STEM can be described as a convolution between the intensity of the electron probe and an object function [11]. Such a description is only possible if there is no coherency between nearby parts of the object. In other words, HAADF-STEM imaging can be described as being incoherent. This incoherent imaging arises on the one hand from the geometry of the detector and on the other hand from contributions of phonon scattering. Because the high angle incoherent scattering gives an intensity which scales approximately with the squared atomic number, the main advantage of working in HAADF-STEM mode is the possibility to visually distinguish between materials with different compositions. This imaging mode is therefore also called *Z*-contrast imaging. [11, 12].

The main purpose of this study is to examine if HAADF-STEM can be used as a sensitive method to identify or at least differentiate between nickel silicides. In order to do this, a set of nickel silicide reference samples is examined: Ni_3Si, $Ni_{31}Si_{12}$, Ni_2Si, NiSi and $NiSi_2$. We use this set of reference samples to define the relationship between the experimental *Z*-intensity and composition. This methodology is then applied to device structures containing various nickel silicides.

Sample preparation and experimental setup

Nickel silicide reference samples are prepared by rapid thermal annealing of a Ni-layer (thickness range from 60 to 170 nm) either deposited directly on a Si(001) substrate, or deposited on a thin polycrystalline Si film (about 100 nm thick) on top of a SiO_2/Si(001) substrate. The temperature and thickness ratio of the Ni and Si layers are varied to obtain different phases. X-ray diffraction (XRD) is used to investigate which phases the samples contain, and the composition of the silicide layers is determined by EDS [9] and EELS [9, 10]. In most cases, the preparation resulted in a layer consisting of a single phase, i.e. Ni_3Si, NiSi or $NiSi_2$. In one case, a layered silicide with two phases is obtained: $Ni_{31}Si_{12}$ and Ni_2Si.

All samples are prepared for TEM in cross section by focused ion beam (FIB, Strata400S) with in situ lift-out. The nickel silicide reference samples are produced in a wedge shape with a thickness gradient to study the effect of specimen thickness on the quantification results. In principle the thickness increases linearly from 0 to $\sim$300 nm, but in practice the thinnest part is rounded due to the ion beam milling. Both the FUSI gate and the tunnel field-effect transistor (TFET) device structures are prepared as plan parallel cross-sectional samples.

HAADF-STEM measurements are carried out on a Tecnai F30 microscope operating at 300 kV. A spot size of about 1–2 nm is used. The HAADF detector semi-angle is 25 mrad. An attempt is made to further exclude diffraction contrast by performing additional measurements with a JEOL 3000F microscope, operating at 300 kV with a detector semi-angle of 30 mrad.

The HAADF-STEM images are processed using FEI TEM Imaging and Analysis (TIA), and Digital Micrograph (DM) software.

Results and discussion

Correlation between HAADF-STEM intensity and sample thickness

Prior to comparing the HAADF-STEM intensities of the nickel silicide reference samples, it is necessary to examine the correlation between sample thickness and experimental HAADF-STEM intensity. In order to study this correlation, wedge-shaped samples of the nickel silicide references, which have a thickness ranging from 0 to about 300 nm, are examined. HAADF-STEM images of these samples are recorded at identical experimental conditions (beam intensity, detector angle, contrast and brightness settings, scan rate, etc.). Figure 1 shows HAADF-STEM images of the different phases at comparable thicknesses. A difference in the intensity of the silicide layers can be seen. The samples are tilted 5° away from the Si [110] zone axis to eliminate channelling of the substrate and of the epitaxial $NiSi_2$ phase. Since most of the layers are polycrystalline, all channelling contrast cannot be suppressed in all grains simultaneously. Intensity profiles are taken on the images, along the silicide layers, using TIA software.

For each nickel silicide phase, the thickness of the sample is measured at 15 points along the wedge-shaped silicide layer, using the EELS log ratio method. This is done with DM software. The dataset is then extrapolated

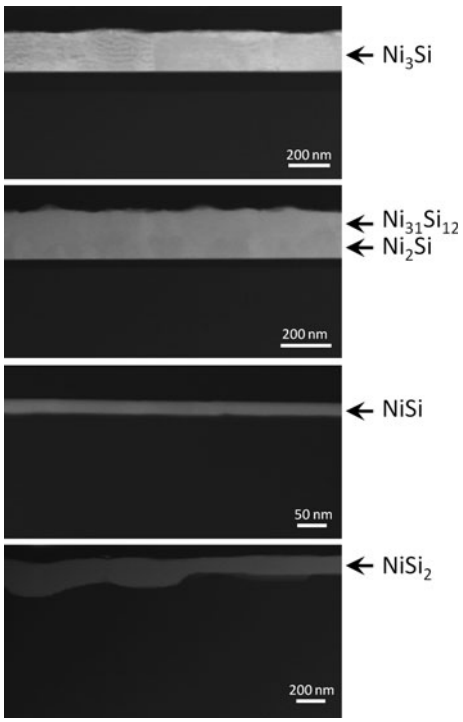

Fig. 1 HAADF-STEM images of the nickel silicide reference samples, taken at identical experimental conditions, at comparable sample thickness ranges increasing from left to right (150–190 nm)

over the entire length of the silicide layer to obtain the thickness at each point. In order to determine the thickness, the total inelastic mean free path, λ, is required. λ is a function of the collection semi-angle, the incident energy and a mean energy loss which depends on the chemical composition of the specimen. Bonney [13] reported that this thickness determination gives values which lie within 10% of the true value, when tested on sub-micron vanadium spheres of which the thickness was taken to be the same as their diameter [13, 14]. Meltzman et al. [15] reported, however, that this error is larger when a high beam energy (i.e. 300 kV) and a large collection angle are used. Furthermore, since the chemical composition of the nickel silicides on the device structures is unknown, a larger error is expected on the thickness determination in the quantification procedure.

The correlation between the intensity profiles and thicknesses is examined. Figure 2 shows that a linear relation is obtained between HAADF-STEM intensity and sample thickness. The intensity profiles shown here are from the $NiSi_2$ (Fig. 2a) and Ni_3Si (Fig. 2b) phases, and from the Si substrate (Fig. 2c). This linear dependence is in agreement with Pennycook and Nellist [11], who have shown that the thickness behaviour of the image intensity changes from oscillatory at low angles reflecting the long coherence length between phonons, to more linear at large angles where the coherence length is much shorter than the

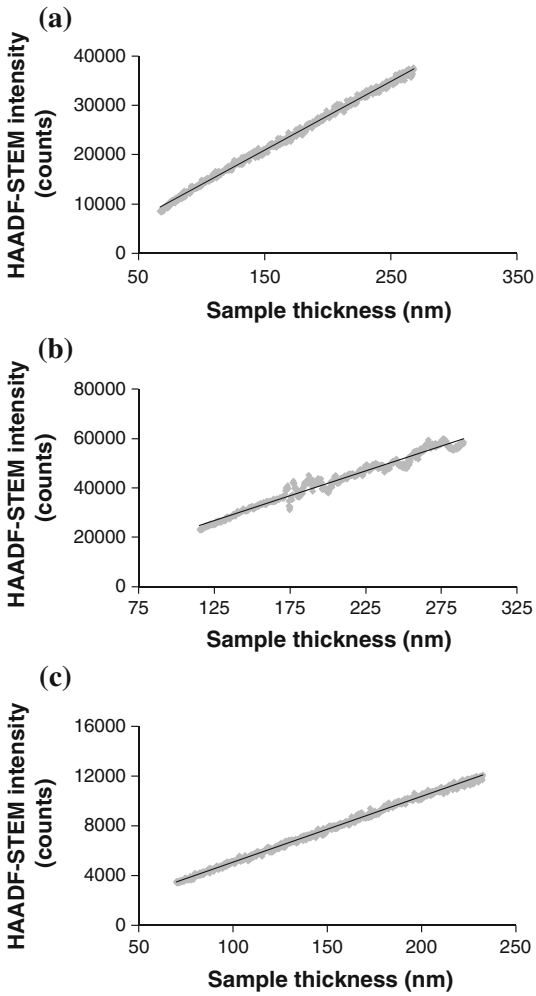

Fig. 2 Correlation between HAADF-STEM intensity and sample thickness for (**a**) the $NiSi_2$ phase, (**b**) the Ni_3Si phase and (**c**) the Si substrate. A linear fit is made through the data points

specimen thickness [11]. This methodology is not applicable at the very thin part of the wedge; since there the thickness interpolation becomes unpredictable.

It can be seen in Fig. 2 that the profile of Ni_3Si shows fluctuations, while the profile of $NiSi_2$ shows smoother thickness dependence. This different behaviour can be attributed to the fact that $NiSi_2$ is grown epitaxial on the silicon substrate, i.e. is single crystalline in the whole studied area, while Ni_3Si is polycrystalline. The fluctuations are due to diffraction contrast that reaches the detector and to electron channelling in the grains. Figure 1 shows that the HAADF-STEM images still show diffraction contrast, even though they are recorded using a high angle annular dark field detector at the largest possible detector angle (in this case, the detector semi-angle equals 25 mrad). It is clear that this will disturb the *Z*-dependence of the image intensity. The influence of diffraction contrast and channelling on the measurements will be discussed further.

Comparison of the reference samples

Because the HAADF-STEM images are taken at identical experimental conditions, the differences in intensity of the nickel silicide phases depend solely on the squared averaged atomic number, the atomic density and the sample thickness. Other factors, such as electron density in the beam, detector angle, can be considered to be constant during the measurements. We can state that:

$$I = cZ^2Nt \quad (1)$$

with I the HAADF-STEM intensity, Z the average atomic number, N the atomic density, t the sample thickness and c a constant. The Z^2 dependence is expected on the basis of Rutherford scattering. Pennycook and Nellist [11] report a dependence which is only slightly less than Z^2 by calculating the dynamical object function for incoherent imaging of thick crystals.

Because the images are taken at lower magnifications with a probe size of about 1–2 nm, the probe function is averaged over the atomic columns. Therefore, we expect that the probe function will not influence the comparison of the intensities of the nickel silicide reference samples.

We will now discuss two methods to remove thickness effects from the intensity profiles. This is necessary to compare the HAADF-STEM intensities of the nickel silicide phases. In the first method, the ratio of the intensity to the sample thickness is determined for each point of the intensity profile. Since there is a linear relationship between intensity (counts) and thickness, this ratio is directly proportional to the squared average atomic number and the atomic density, in agreement with Eq. 1. Subsequently, the mean of these values is determined. This is done for each phase. The means together with the standard deviations are given in Table 1. In Fig. 3a, these values are plotted versus Z^2N calculated based on composition and crystallographic structure. It can be seen that a linear relation is obtained, which is as expected because Z^2N should scale with the HAADF-STEM intensity. The error bars are given by the standard deviations. It is clear

Table 1 HAADF-STEM intensities of the nickel silicide reference samples relative to the sample thickness and the intensity of the silicon substrate. The values are compared to Z^2N, calculated based on composition and crystallographic structure

Phase	Z^2N ($\times 10^{25}$/cm^3)	$I_{(\text{nickel silicide})}/t$ (counts/nm)	$I_{(\text{nickel silicide})}/I_{(\text{Si})}$
$NiSi_2$	2.66	139.8 ± 2.9	3.5 ± 0.2
NiSi	3.66	160.2 ± 5.0	4.4 ± 0.2
Ni_2Si	4.99	184.1 ± 5.1	5.7 ± 0.3
$Ni_{31}Si_{12}$	5.28	199.0 ± 6.1	5.9 ± 0.4
Ni_3Si	5.70	208.6 ± 8.4	6.3 ± 0.3

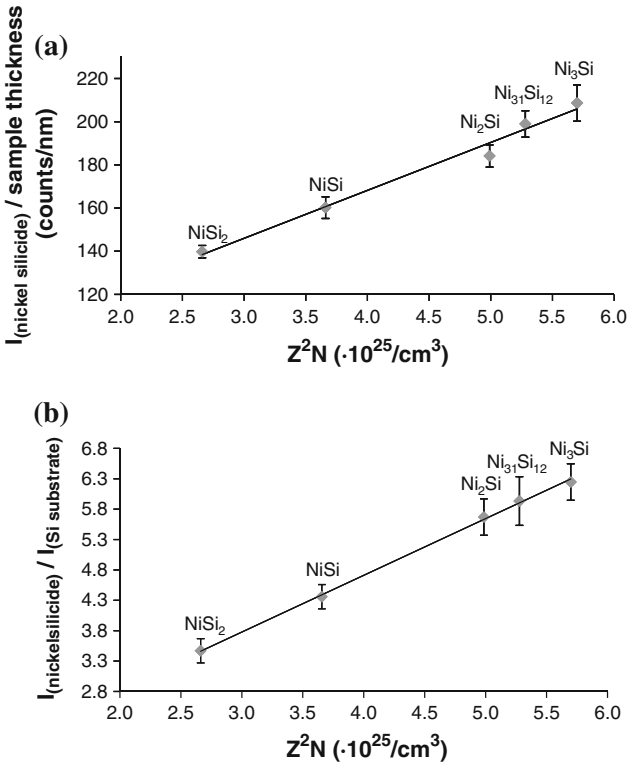

Fig. 3 Ratio of HAADF-STEM intensity relative to (**a**) the sample thickness (nm) and (**b**) the intensity of the silicon substrate for equal specimen thickness. A linear fit is made through the data points

that the $NiSi_2$ and NiSi phases can be unambiguously distinguished from the other phases. However, the more nickel-rich silicides, Ni_2Si, $Ni_{31}Si_{12}$ and Ni_3Si, are more difficult to distinguish.

The thickness normalized intensities can change over time mainly due to differences of the beam current used and the HAADF-detector sensitivity. This implies that to obtain a high precision, the set of nickel silicide reference samples will have to be re-measured each time an unknown sample is examined. Moreover, apart from the simple acquisition of a HAADF-STEM image of the sample of interest, cumbersome thickness measurements will be necessary. Since this is impractical for a fast quantitative analysis, an alternative methodology is proposed. The HAADF-STEM intensities can be scaled by the intensity of the silicon substrate acquired at a position with the same foil thickness as the silicide. This way, the change of the relative intensities over time due to changes in experimental conditions, is omitted. In this methodology, it is assumed that the nickel silicide layers and silicon substrate are thinned equally by the FIB sample preparation procedure. As the ion beam in the FIB is incident under grazing angle, no large thickness steps are expected between the silicide and the underlying substrate.

The ratio of the HAADF-STEM intensities relative to the intensity of the silicon substrate as a function of the squared atomic number and atomic density is shown in Fig. 3b and Table 1. The error bars are given by the standard deviations. It can be seen that, using this methodology, again a linear relationship between the relative HAADF-STEM intensity and Z^2N is obtained. As with the previous methodology, the $NiSi_2$ and NiSi phases can be well distinguished from the other phases. The error bars of the more nickel-rich silicides (Ni_2Si, $Ni_{31}Si_{12}$ and Ni_3Si) overlap. In order for the quantification procedure to be successful, the TEM-specimen thickness in the silicon substrate should not differ more than about 10% from the thickness in the silicide layer, based on the obtained means and standard deviations. This condition is generally fulfilled on FIB prepared specimens.

Both methodologies allow us to quantify the relationship between the experimental *Z*-contrast intensities and composition of the analysed nickel silicide samples. The phases follow the expected trend that a higher nickel concentration corresponds with a higher relative intensity.

Influence of diffraction contrast and channelling

It is expected that only high angle incoherent scattering is recorded with the HAADF detector. Nevertheless, it can be seen on Fig. 1 that diffraction contrast is still visible, even though the images are recorded with the HAADF-detector set at the largest detector angle. It is clear that this can disturb the Z^2 dependence of the image intensity. The influence of diffraction contrast on the quantification results is illustrated by Fig. 2, where the intensity profile of polycrystalline Ni_3Si is compared to the intensity profile of epitaxial $NiSi_2$. The fluctuations in intensity caused by diffraction contrast will affect the standard deviations of the intensities of the reference samples. An attempt is made to overcome the diffraction contribution to the image intensity by re-performing the second quantification procedure using relative intensities, with a larger detector angle (30 mrad) in a JEOL 3000F microscope. Figure 4 shows that, even though the standard deviations are smaller than with the 25 mrad detector semi-angle (Fig. 4b), diffraction effects can, also in this case, not completely be omitted (Fig. 4a).

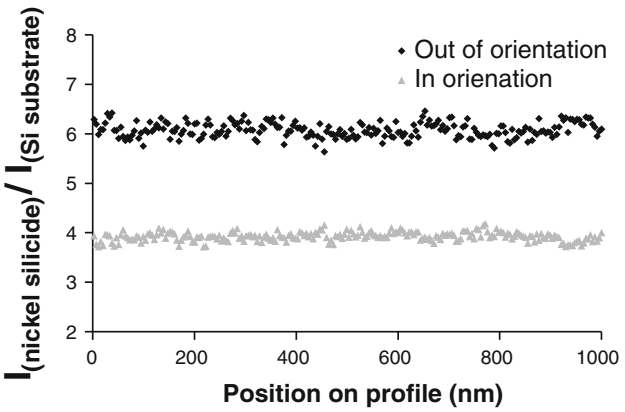

Fig. 5 Influence of channelling on the quantification methodology. Intensity profiles of a part of the Ni_3Si layer are shown in [110] zone axis orientation and tilted 5° away from this orientation

Figure 5 demonstrates the effects of channelling, by comparing the relative intensity of the Ni_3Si phase when the Si substrate is oriented along the [110] zone axis, with the relative intensity of the Ni_3Si phase when tilted 5° out of orientation. When the Si substrate is oriented along a zone axis, a higher Si intensity is measured on the HAADF-STEM detector which leads to a lower relative intensity for the silicide. The 5° tilt away from the zone axis is typically used during all our measurements, to avoid channelling effects in the Si substrate. In the relatively thick blanket layers used as reference samples this tilt is generally not a problem, but in device structure with thin layers and narrow structures this might limit the lateral resolution that can be obtained due to overlap with neighbouring materials.

Application on transistor structures

The validity of the quantification methodology is evaluated on device structures which contain different nickel silicide phases. The quantification methodology is applied to TFETs and CMOS device structures with FUSI gates.

The TFETs are promising successors of metal–oxide–semiconductor FETs (MOSFETs). The TFETs major

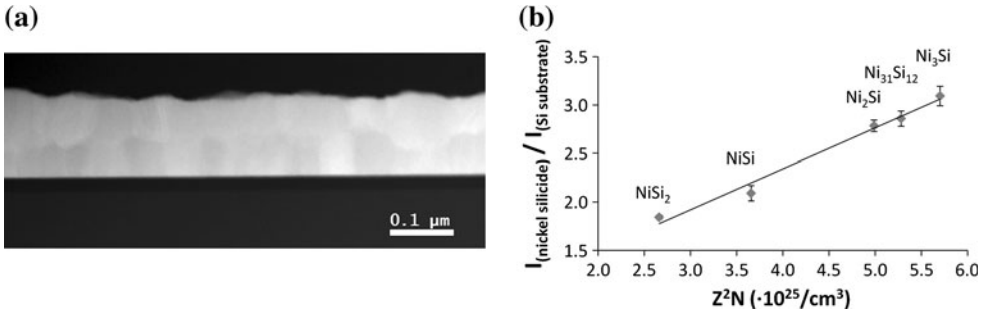

Fig. 4 Measurements with a JEOL 3000F microscope at a detector semi-angle of 30 mrad. (**a**) HAADF-STEM image of the sample containing $Ni_{31}Si_{12}$ and Ni_2Si. Diffraction contrast is still visible. (**b**) Relative intensity ratios for the different reference samples

advantage is a significant decrease in power consumption [16–19]. Due to this decreased power consumption, TFET process integrations allow an increased on-chip device density compared to the MOSFET, a benefit which can be especially exploited in vertical nanowire-based transistor architectures with three-dimensional stacking capability. The structure investigated here is a planar TFET structure obtained by applying different dopant implantations in source and drain region. The edge of the implantation mask is nearly in the middle of the gate. For the given annealing conditions, the silicidation turned out to be non-uniform and dependent on doping and width of the active region. TEM images of such structures with different gate dimensions are shown in Fig. 6. Figure 6a illustrates the dependence on the active width (all regions are n-type in this test structure), Fig. 6b the effect of different doping of source versus drain. The specimens are thinned by FIB and are tailored to have a constant thickness. Slight thickness variations occur due to variations in milling rates of the different materials ("curtaining", see e.g. the darker contrast in the oxide under the W-filled contacts on the TEM image in Fig. 6b). Prior to applying the HAADF-STEM quantification procedures, the samples are examined by EDS using the absorption corrected Cliff–Lorimer approach [20, 21]. The results of the EDS analyses, together with the expected phases are given in Table 2. The quantification procedure relating the HAADF-STEM intensity to the sample thickness is applied to the transistor structures. The results are given in Table 2 and can be compared to the reference samples in Table 1. However, due to differences in the beam current and the HAADF-detector sensitivity on the one hand, and the relatively large error on the thickness measurements on the other hand, the obtained values are generally too small when compared to the reference samples.

Subsequently, the mean intensity relative to the intensity of the Si substrate is determined for the HAADF-STEM images and is given both in Table 2 and by the 2D colour maps in Fig. 6. The choice of the Si region to scale the image does not have a significant influence on the quantification results, as long as there are no large differences in thickness. The Si region for the normalisation is chosen outside the area with some curtaining, as is indicated by the boxes on the 2D colour maps. The obtained values are

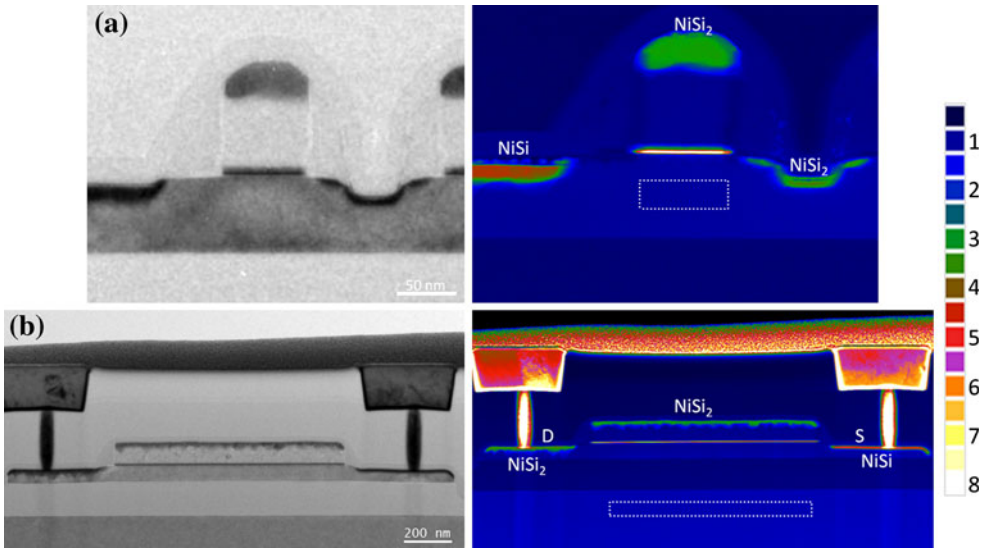

Fig. 6 TEM images and corresponding HAADF-STEM 2D colour maps normalized to the Si substrate (*box*) of TFET device structures (colours can be seen online) (**a**) test structure with dense lines, the *outer line* is shown, i.e. on the left a wide silicided area is present, (**b**) TFET, source and drain regions are indicated by *S* and *D*, respectively

Table 2 Application of the quantification methodology on TFET device structures. The compositions determined by EDS are presented. The Si concentrations are given in atomic percentages

Position	EDS (at.% Si)	Phase based on EDS	$I_{(\text{nickel silicide})}/t$ (counts/nm)	$I_{(\text{nickel silicide})}/I_{(\text{Si})}$
Figure 6a, gate	67.0 ± 1.8	$NiSi_2$	119.6 ± 2.1	3.6 ± 0.1
Figure 6a, left	51.4 ± 0.8	NiSi	140.1 ± 3.2	4.4 ± 0.2
Figure 6a, right	67.8 ± 1.5	$NiSi_2$	118.5 ± 2.5	3.4 ± 0.1
Figure 6b, gate	65.3 ± 0.8	$NiSi_2$	110.6 ± 1.6	3.7 ± 0.1
Figure 6b, source	49.0 ± 2.2	NiSi	166.0 ± 3.2	4.3 ± 0.2
Figure 6b, drain	66.1 ± 2.8	$NiSi_2$	112.6 ± 3.4	3.7 ± 0.2

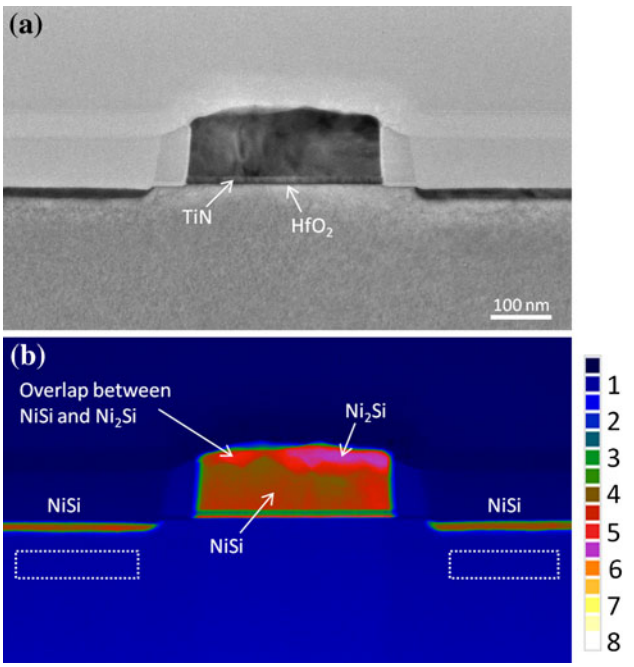

Fig. 7 (**a**) TEM image and (**b**) corresponding HAADF-STEM 2D intensity colour map normalized to the Si substrate (*boxes*) of a FUSI device structure (colours can be seen online)

Table 3 Application of the quantification methodology on a FUSI device structure. The compositions determined by EDS are presented. The Si concentrations are given in atomic percentages

Position	EDS (at.% Si)	Phase based on EDS	$I_{(\text{nickel silicide})}/I_{(\text{Si})}$
Gate top	32.3 ± 1.2	Ni_2Si	5.4 ± 0.1
Gate bottom	49.2 ± 2.0	NiSi	4.2 ± 0.1
Left	50.7 ± 2.7	NiSi	4.2 ± 0.1
Right	50.6 ± 2.5	NiSi	4.2 ± 0.1

compared to the reference values to determine the nickel silicide phases, which are then indicated on Fig. 6. It can be seen that the quantification results match well with the EDS quantifications. In the regions of the devices where silicide is expected, the 2D colour maps allow to immediately distinguish between the silicide phases. The colour changes at the edges of the silicided regions are due to projected roughness. The edges appear as more Si-rich regions, which are caused by overlap of the silicide and Si.

The quantification methodology is also applied to CMOS device structures with FUSI gates [3, 4]. Figure 7a shows a TEM image of a FUSI device structure with multiple nickel silicides in the metal gate, which is formed on a 10 nm TiN/1.5 nm HfO_2 stack. The 2D HAADF-STEM colour map (Fig. 7b) is obtained by performing the quantification methodology using relative intensities. The intensity is normalized by the average of the silicon intensities in the marked boxes. EDS measurements performed on these samples are given in Table 3, together with the results of the STEM quantification methodologies. The phases are also indicated on Fig. 7b. It is shown that the EDS results match well with the HAADF-STEM quantification results. We can conclude that the gate contains both the Ni_2Si (top part) and the NiSi (bottom part) phases. It can be seen on Fig. 7b that the two phases overlap on the top left part of the gate.

These two examples demonstrate that a fast 2D quantitative compositional analysis based on HAADF-STEM image intensity is possible. The distribution of the silicides can be well visualized on the false colour images. The method is especially efficient for identification of the silicon-rich nickel silicide phases ($NiSi_2$ and NiSi) whereas the metal rich phases are more difficult to distinguish. It is shown that the quantifications by HAADF-STEM and EDS correspond very well.

Conclusions

It is shown that HAADF-STEM imaging can be used as a sensitive method for the identification of nickel silicides. A quantification methodology is developed by examining a set of nickel silicide reference samples with known composition. It is demonstrated that a linear correlation exists between HAADF-STEM intensity and sample thickness. Normalizing the experimental intensities of the reference samples to the measured sample thickness is a possible path for quantification. However, in order to obtain high precision over longer time, the regular re-measurement of the reference samples is necessary. Moreover, thickness measurements have to be done in the regions of interest of each analysed unknown structure. As a consequence, this method is time consuming. A faster quantification method is proposed, in which the ratio of the intensities of the silicided regions to the intensity of the underlying silicon is determined. It is shown that the Si-rich nickel silicide phases ($NiSi_2$ and NiSi) can clearly be distinguished in the quantification. The more nickel-rich silicides (Ni_2Si, $Ni_{31}Si_{12}$ and Ni_3Si) show overlap in their standard deviations. It is demonstrated that this methodology can successfully be applied to device structures to identify the nickel silicide phase distribution. The use of 2D colour maps is illustrated. Knowing where the silicides are expected, the 2D maps allow a fast visualisation of the distribution of the different phases.

Acknowledgements The authors would like to thank Daniele Leonelli (Imec, Leuven) for providing the TFET structures, Lars-Ake Ragnarsson (Imec, Leuven) for the FUSI structures, Jo Verbeeck

(EMAT, Universiteit Antwerpen) for HAADF-STEM measurements with the JEOL 3000F microscope, Paola Favia (Imec, Leuven) for discussion on the STEM analysis and DM software, and Patricia Van Marcke (Imec, Leuven) for sample preparations.

References

1. Maex K, Van Rossum M (1995) Properties of metal silicides. INSPEC, London
2. Maex K (1993) Mater Sci Eng R11:53
3. Kittl JA, Lauwers A, van Dal MJH, Yu H, Veloso A, Hoffmann T, Pawlak MA, Demeurisse C, Kubicek S, Niwa M, Vrancken C, Absil P, Biesemans S (2006) ECS Trans 3:233
4. Kittl JA, O'Sullivan BJ, Kaushik VS, Lauwers A, Pawlak MA, Hoffmann T, Demeurisse C, Vrancken C, Veloso A, Absil P, Biesemans S (2007) Appl Phys Lett 90:032103
5. Gambino JP, Colgan EG (1998) Mater Chem Phys 52:99
6. Lavoie C, d'Heurle FM, Detavernier C, Cabral C (2003) Microelectron Eng 70:144
7. Shiojiri M, Yamazaki T (2003) Jeol News 38(2):54
8. Watanabe K, Yamazaki T, Kikuchi Y, Kotaka Y, Kawasaki M, Hashimoto I, Shiojiri M (2001) Phys Rev B 63:085316
9. Verleysen E, Bender H, Schryvers D, Vandervorst W (2010) J Phys Conf Ser 209:012057
10. Verleysen E, Bender H, Richard O, Schryvers D, Vandervorst W (2010) J Microsc 240:75. doi:10.1111/j.1365-2818.2010.03391.x
11. Pennycook SJ, Nellist PD (1999) Impact of electron microscopy on materials research. Kluwer Academic, Dordrecht
12. Pennycook SJ, Jesson DE (1991) Ultramicroscopy 37:14
13. Bonney LA (1990) In: Proceedings of the XIIth international congress for electron microscopy. San Francisco Press, San Francisco, p 74
14. Egerton RF (1986) Electron energy loss spectroscopy in the electron microscope. Plenum Press, New York
15. Meltzman H, Kauffmann Y, Thangadurai P, Drozdov M, Baram M, Brandon D, Kaplan WD (2009) J Microsc 236:165
16. Leonelli D, Vandooren A, Rooyackers R, Verhulst AS, De Gendt S, Heyns MM, Groeseneken G (2009) In: Extended abstracts solid state devices and materials conference, p 767
17. Leonelli D, Vandooren A, Rooyackers R, Verhulst AS, De Gendt S, Heyns MM, Groeseneken G (2010) Jpn J Appl Phys 49: 04DC10
18. Verhulst AS, Vandenberghe WG, Leonelli D, Rooyackers R, Vandooren A, De Gendt S, Heyns MM, Groeseneken G (2009) ECS Trans 25:455
19. Verhulst AS, Sorée B, Leonelli D, Vandenberghe WG, Groeseneken G (2010) J Appl Phys 107:024518
20. Cliff G, Lorimer GW (1975) J Microsc 103:203
21. Williams DB, Carter CB (1996) Transmission electron microscopy. Plenum Press, New York